mmSense: Multi-Person Detection and Identification via mmWave Sensing

Tianbo Gu, Zheng Fang, Zhicheng Yang, Pengfei Hu, and Prasant Mohapatra
Department of Computer Science, University of California, Davis, CA, USA
{tbgu,zkfang,zcyang,pfhu,pmohapatra}@ucdavis.edu

ABSTRACT

In recent years, millimeter-wave (mmWave) is becoming a significant component of the next-generation wireless communication due to its up to 7 Gbps transmission rate. In addition to the communication benefits, the unique sensing feature of mmWave attracts more attention. Nowadays, the services of human detection and identification are needed in numerous application scenarios, such as smart home and smart industry. The RF-based sensing techniques, especially WiFi-based, are widely utilized in human detection and identification. However, these work either require humans to carry devices or cannot detect and identify multiple people simultaneously.

In this paper, we propose *mmSense*, a device-free multi-person detection and identification framework, which exploits the unique mmWave sensing features. First, we utilize the properties of directionality, impenetrability, and reflection of 60 GHz signal for objects to fingerprint the environments. Based on the generated environment fingerprints with and without human presence, *mmSense* can detect and localize the presence of multiple people simultaneously via the LSTM-based classification model. Moreover, we propose a novel approach to use humans' outline profile and vital signs to identify multiple people by using 60 GHz reflected signals of the human body. We conduct extensive experiments to demonstrate the low-cost and effectiveness of our approach.

CCS CONCEPTS

• **Human-centered computing** → **Mobile computing**; • **Networks** → *Wireless local area networks*;

KEYWORDS

Millimeter wave; Human detection; Human identification; Localization; 60 GHz sensing; Vital signs; Deep learning

mmNets'19, October 25, 2019, Los Cabos, Mexico

ACM ISBN 978-1-4503-6932-9/19/10…$15.00
https://doi.org/10.1145/3349624.3356765

ACM Reference Format:
Tianbo Gu, Zheng Fang, Zhicheng Yang, Pengfei Hu, and Prasant Mohapatra. 2019. mmSense: Multi-Person Detection and Identification via mmWave Sensing. In *3rd ACM Workshop on Millimeter-wave Networks and Sensing Systems (mmNets'19), October 25, 2019, Los Cabos, Mexico.* ACM, New York, NY, USA, 6 pages. https://doi.org/10.1145/3349624.3356765

1 INTRODUCTION

Nowadays, the broad deployment of the Internet of Things (IoT) is changing the world and makes human's lives more convenient. Human is always the core element considered in the design of IoT. Human detection and identification are essential functions in IoT applications. For instance, in smart homes, the detection of human presence enables the automation of a variety of indoor applications. One typical application is that the automatic room temperature adjustment based on humans' presence. For the elderly, continuously monitoring their locations and behaviors could help to detect some emergency cases, such as a long stay in the bathroom due to suddenly falling. For smart building, the detection of human and estimation of room occupancy is of particular importance, which can be used to dynamically adjust the heating, ventilation, and air-conditioning (HVAC) facilities to reduce energy consumption. However, the existing approaches are facing many challenges.

First, some works require humans to carry a particular device to assist the detection of presence. However, it is infeasible to request everybody to wear such a device at any time in most scenarios, such as human detection in a shopping mall. Thus, device-free based solutions, such as WiFi sensing, are adopted widely to detect humans and even their gestures. But they either require the human to continuously move to detect his presence or they need to conduct a lot of preliminary measurement and profiling with manual intervention in a strict controlled-environment.

Furthermore, the current most solutions cannot support multi-person detection and identification. The channel state information (CSI) [11, 19] from the WiFi signal can be utilized to detect and identify one single person. However, the multi-path effect introduced by a complex indoor environment makes it challenging to establish an accurate model to distinguish and detect multi-person simultaneously. Other additional Non-intrusive information, such as electrical energy demand, water consumption, and various indoor IoT sensors are used to enhance the accuracy of human presence

detection [3, 7]. But this also increases the complexity of human detection and localization and cannot implement the detection in a real-time fashion.

Recently, 60 GHz communication, as the most crucial next-generation wireless communication technique, is widely adopted due to its extraordinary data rate (up to 6.7 Gbps). 60 GHz's short wavelength leads to an excellent sensing capability. The increasingly widespread deployment of mmWave communication also provides us the feasibility and availability to use the mmWave for sensing. In this paper, we propose *mmSense*, a device-free multi-person detection and identification approach via mmWave sensing. The *contributions* of our work are as follows:

- We use the properties of directionality, impenetrability, reflection, and scattering of 60 GHz signal for objects and human bodies to fingerprint the environments with and without human presence. The designed fingerprinting method can be done automatically without human intervention.
- Based on the monitored 60 GHz signals and generated fingerprints of environments, *mmSense* can detect the presence of multi-person humans and their locations simultaneously via the LSTM-based classification model. Our model can be tuned automatically without the need of professional experiences to select the features manually.
- We put forward a novel approach to construct the human outline and measure the humans' vital signs via the 60 GHz reflected signals. We correlate the 60 GHz RSS series with the measurement of different people's outlines and vital signs to identify the humans.
- We design extensive experiments to demonstrate the low-cost and effectiveness of our human detection and identification mechanism. Our method can be widely applied for practical scenarios and facilitate the current research in both human detection and identification.

2 HUMAN DETECTION AND IDENTIFICATION

2.1 System overview

In this work, we propose a novel multi-person detection and identification system. First, the system tries to learn the environments and construct the fingerprints of environments with and without human presence. The unique directionality, impenetrability, reflection, and scattering characteristics of 60 GHz signals for diverse objects and human bodies can be used to generate the fingerprints. Based on the generated fingerprints of environments, we use the LSTM-based classification model to detect the human presence and their locations. Compared to the traditional WiFi-based localization fingerprinting, our approach does not need human intervention and can be done automatically. By utilizing environment segmentation and spatial isolation of the 60 GHz signal, our system can detect multiple people and their locations simultaneously.

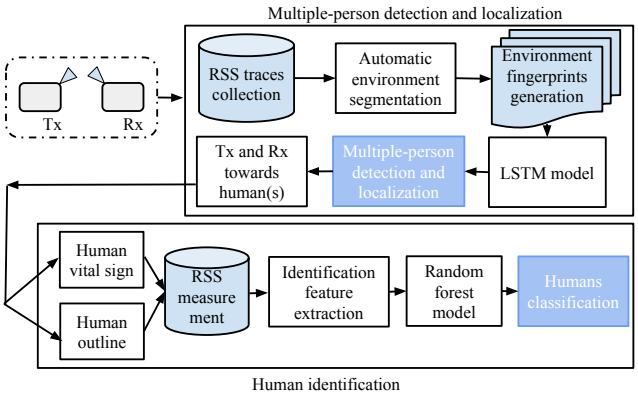

Figure 1: Overview of *mmSense*

Once we can detect humans' presences and their locations, the system will adjust their Tx and Rx beams to the human body and tried to identify the humans based on the reflected 60 GHz signal from the human body. We propose a novel research direction that uses the human outline and vital signs to identify humans. The collected reflected RSS series can be used to construct the human outline and analyze human's vital signs, which form the unique feature set to identify the humans. The procedures our human detection and identification are displayed in Figure 1.

2.2 Environment and human body reflection model

First, we build the reflection model of objects and human bodies, which is used for the generation of environment fingerprints. For a pair of Transmitter (Tx) and Receiver (Rx), the path loss PL can be calculated as follows:

$$PL = L_d + L_{Rl} = 20log(\frac{4\pi d}{\lambda}) + L_{Rl} \quad (1)$$

where L_d and L_{Rl} are the signal attenuation of distance d and signal reflection loss. The reflection loss L_{Rl} is related to the reflection coefficient ϑ of objects. We use P_{ar} and P_{br} to denote the values of reflected (after reflection) and incident (before reflection) power. Then the L_{Rl} can be calculated as follows:

$$L_{Rl} = \frac{P_{ar}}{P_{br}} = |\vartheta|^2 = |\frac{1-e^{-j2\varepsilon}}{1-\vartheta_i'^2 e^{-j2\varepsilon}}\vartheta_i'|^2, \text{for i} \in \{\perp, \|\} \quad (2)$$

where $\varepsilon = \frac{2\pi l}{\lambda}\sqrt{\xi_2/\xi_1 - sin^2\theta}$. l, λ and θ are the thickness of the reflecting source, signal wavelength and the incident angle. ξ_1 and ξ_2 represent the permittivities of first and second transmission medium. $\vartheta_\perp$ and $\vartheta_\|$ are the Fresnel's reflection coefficients [2] when the electric field is perpendicular and parallel to the incidence plane.

In addition to the reflection, the roughness of object surface may produce scattering effect. Then the incident power is distributed over the specular direction. The roughness of an object surface can be determined by the Rayleigh criterion as $h' = \lambda/(8cos\theta)$. The object surface is considered to be rough if the height h of a given surface is larger than h', otherwise,

it is smooth. The scattering loss factor ε_s with the standard deviation of surface height σ_h will be denoted by:

$$\varepsilon_s = exp\left[-8(\frac{\pi\sigma_h cos\theta}{\lambda})^2\right] \quad (3)$$

Then the Fresnel reflection coefficients are modified by:

$$\{\vartheta_\perp, \vartheta_\parallel\}_{rough} = \varepsilon_s \cdot \{\vartheta_\perp, \vartheta_\parallel\} \quad (4)$$

2.3 Multi-person detection and localization

In this work, we consider a typical indoor mmWave communication deployment, where there are one Tx and multiple Rx. The Tx is usually placed in a fixed location and works as a router. The Rx could be a variety of electronic devices that request high-speed wireless access, such as the television, desktop computer, and camera. Our approach can be easily extended to multiple Tx if one Tx cannot cover all the signal transmission areas.

Fingerprints generation. Our goal is to detect multi-person and obtain their locations. The variation of the reflected signal from the environment could imply the appearance of humans. To detect the presence of multi-person, we propose to segment the environment into different areas. Initially, *mmSense* system is unacquainted with the environment and does know nothing. Based on the angle of departure (AoD) of signal from Tx, the environment is segmented into K fine-grained areas $\mathcal{A} = \{\mathcal{A}_1, ..., \mathcal{A}_k, ..., \mathcal{A}_K\}$. For a specific beam width w, area $\mathcal{A}_k$ can be covered by a beam angle set from the Tx side:

$$\Lambda^{\mathcal{A}_k} = \{\Lambda_1^{\mathcal{A}_k}, \Lambda_2^{\mathcal{A}_k}, ..., \Lambda_a^{\mathcal{A}_k}\} \quad (5)$$

which also corresponds to certain beam sectors of transmission. For the Rx side, suppose we have M receivers $\{R_1, ..., R_m, ..., R_M\}$. The angel of arrival (AoA) of signal for receiver R_m could be represented as:

$$\Lambda^{R_m} = \{\Lambda_1^{R_m}, \Lambda_2^{R_m}, ..., \Lambda_b^{R_m}\} \quad (6)$$

Then, there are $a \times b$ transmission paths (beam sectors pairs) TP between Tx and Rx R_m:

$$TP_i \in BS_{R_m}^{\mathcal{A}_k} = \Lambda^{\mathcal{A}_k} \times \Lambda^{R_m} \quad (7)$$

Instead of line-of-sight (LOS), we only consider the non-line-of-sight (NLOS) transmissions paths. The signal variations of NLOS resulting from the reflection of diverse environmental surfaces can be used to fingerprint the environments.

According to Equation 1, the received signal strength (RSS) loss for transmission path TP_i could be denoted as:

$$RSS_{R_m}^{TP_i} = -PL(d, \vartheta, \theta) \quad (8)$$

For each path, the RSS may be distinct due to different transmission distance d, reflection coefficient ϑ and incident angle θ. For the area $\mathcal{A}_k$, all the transmission paths from K receivers can be denoted via:

$$BS^{\mathcal{A}_k} \doteq \{BS_{R_1}, ..., BS_{R_M}\} = \{\Lambda^{\mathcal{A}_k} \times \Lambda^{R_1}, ..., \Lambda^{\mathcal{A}_k} \times \Lambda^{R_M}\} \quad (9)$$

In order to capture the spatial and temporal characteristics of reflected signal from environment, Tx rotates to scan the area $\mathcal{A}_k$ starting from beam angle $\Lambda_1^{\mathcal{A}_k}$ to $\Lambda_a^{\mathcal{A}_k}$. Each receiver R_m monitors the reflected signals at an AoA $\Lambda_i^{R_m}$ and record the n_i sequential RSS values $\{RSS_1^{\Lambda_i^{R_m}}, RSS_2^{\Lambda_i^{R_m}}, ..., RSS_{n_i}^{\Lambda_i^{R_m}}\}$. We combine the monitored RSS sequences from multiple AoAs and build a new RSS sequence:

$$\overrightarrow{RSS} = \{(RSS^{\Lambda_1^{R_m}}, ..., RSS^{\Lambda_b^{R_m}}), m \in \{1, ..., M\}\} \quad (10)$$

Then we obtain a matrix from multiple receivers from R_1 to R_M that represents the fingerprints of area $\mathcal{A}_k$:

$$F^{\mathcal{A}_k^i} = \begin{array}{c} \begin{matrix} R_1 & \cdots & \cdots & R_M \end{matrix} \\ \begin{pmatrix} RSS_{11} & RSS_{12} & \cdots & RSS_{1M} \\ RSS_{21} & RSS_{22} & \cdots & RSS_{2M} \\ \vdots & \vdots & \ddots & \vdots \\ RSS_{n1} & RSS_{n2} & \cdots & RSS_{nM} \end{pmatrix} \end{array} \quad i \in \{0, 1\}$$

The environment may contain humans or not. For an area $\mathcal{A}_k$, we use $\mathcal{A}_k^1$ to indicate that one person appear in this area, and use $\mathcal{A}_k^0$ to indicate the area is empty.

LSTM-based human detection model. If we initially segment the environment into K areas, we have $2 \times K$ labels that show the state of the areas. We model this problem as a classification problem by establishing the dependency between 60 GHz signal fingerprints and the state of different areas. Therefore, the inputs to the model are RSS matrix F, and the outputs of the model are the area indexes and their states.

To exploit the spatial and temporal features of the data, we employ long short-term memory (LSTM) neural network. Because the LSTM model can retain information across hundreds of time steps, the temporal dependencies of the data can be exploited. Furthermore, the *forward* LSTM contextualizes the current time-step based on those it has seen previously and is inherently suitable for real-time applications.

Due to the initial fine-grained environment segmentation, some continuous areas, such as $\{\mathcal{A}_i, \mathcal{A}_{i+1}, ..., \mathcal{A}_j\}$, may be covered by one human. Then we can merge these areas into one new area and re-segment the environments based on human presence. The automatic environment segmentation can reduce the cost of training and testing of our LSTM-based model for the future human detection and localization.

2.4 Human identification

Human identification is an important research direction because it has relations with many applications in various scenarios, such as user authentication in a smart home. Therefore, after detecting the presence of humans and localizing their positions, *mmSense* adjusts its Tx and Rx beams towards human(s) and tries to identify the humans further.

In this work, we propose to use mmWave sensing technique to identify humans. The proposed approach can discover a rich set of human properties, including human outline and vital signs. By measuring the reflected signals from the human body, we can correlate the RSS series and human properties. Next, we provide the feature set of human properties and discuss how *mmSense* uses them for human identification.

Body surface boundary. The human body can be characterized by multiple dimensions. As shown in Figure 2, the

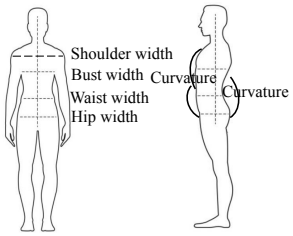

Figure 2: Human outline features.

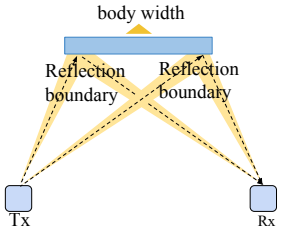

Figure 3: Body width measurement.

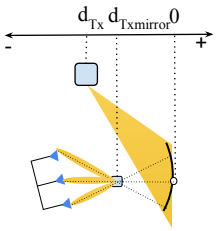

Figure 4: Concave body surface.

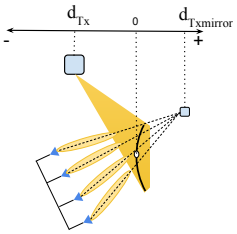

Figure 5: Convex body surface.

shape of a human outline can be reflected by the mutative body widths in the vertical plane. The typical widths of *shoulder, bust, waist, and hip* for people are different. These values of widths can be used to build the *front view* of a human outline. By exploiting the unique effect of 60 GHz directionality on signal reflection, we can detect the body surface boundary. Figure 3 shows that how we measure the widths for the human body. Within the same plane, when Tx moves its beam to cover the inside of the body area, the Rx can align its beam to receive the reflected signals. When Tx moves outside the body area, the reflecting medium of the body disappears, and the Rx cannot receive any signals. Thus, based on the reflected signal, we can find two boundary points that can be used to compute the width. We could use the same method to measure the body widths in the vertical plane. Then we can construct the front view of the human body. What we measure here are not the *real* body widths. Due to the change of the distance between the Tx and the human body, the values may also be different. So we use the *scale values* among widths to identify the person.

Body surface curvature. From the side view of body in Figure 2, we can find the human body surface is curved, either convex or concave. Figure 4 and 5 shows the reflected signal of concave and convex body surface. The focal point Tx_{mirror} can be located via intersecting the reported AoAs. Following the mirror and lens equations, a surface's curvature type is determined by its focal length f:

$$\frac{1}{f} = \frac{1}{d_{Tx}} + \frac{1}{d_{Tx_{mirror}}} \tag{11}$$

where d_{Tx} and $d_{Tx_{mirror}}$ are defined in Figure 4 and 5. The surface is convex if $f > 0$, concave if $f < 0$ and plane if $f \to \infty$. $|f|$ is half of the curvature radius. If Tx sends the signal to the curved surface, the received reflected signal of Rx will be diverse with different values of f. We can correlate the reflected RSS values and f to compute the curvatures of different body areas. These values of curvatures could also be used to identify the humans.

Vital signs. The vital signs can also be utilized to identify humans. The research work in [17] shows that we can measure human's breathing and heart rates via the reflected 60 GHz signals. By directing the Tx and Rx beams to the chest, the tiny chest movements due to the breath and heartbeat can be reflected by the sequential RSS values. In addition to the respiratory rate and heart rate, chest motion patterns from persons, such as amplitude, are also distinct, which can also be used to identify humans.

The body surface boundary, curvature, and vital signs build s robust futures set to identify a person. By continually recording the RSS reflected signals from these dimensions, we can build the fingerprints and use a classical classification algorithm, such as random forest, to classify the humans.

3 EVALUATION

60 GHz sensing platform. We build a customized 60 GHz sensing platform to conduct the experiments. Figure 6 illustrates the key components of the system. At the transmitter side, a Keysight EXG N5172B signal generator provides 10 MHz baseband signals. The signals are then up-converted to 60 GHz by the VubIQ 60 GHz front-end. At the receiver side, the signals are first down-converted to the baseband signals, then fed to a spectrum analyzer (Keysight EXA N9010A) to obtain the real-time measurement of the channel's RSS by calculating the power spectral density distribution. In order to emulate the electronic phased-array based beam steering, we deploy programmable motorized rotators at both transmitter and receiver sides.

Human detection and localization. To prove the effectiveness of our human detection and localization approach, we select one typical indoor office room and design extensive experiments to evaluate our approach. The layout of the indoor environment is shown in Figure 7. This indoor environment consists of a variety of reflection mediums, such as wall, conference TV, whiteboard, metal bookshelf, etc. Other kinds of objects, such as desktop and printer, can also be the objects to influence the reflected signals. Instead of the disadvantages of the complicated environment in WiFi-sensing, the more complicated environment will increase the accuracy of our environment fingerprinting. We show the fingerprints we describe in Equation 10 of three areas with and without human presence in Figure 8. Each area is covered by a sector of angle 40°. From the figure, we can see that sequential RSS values are distinguishable in human's presence and absence scenarios. In Figure 8a, there are two peaks because the presence of human body extend the reflecting medium and form the second signal peak. But in Figure 8b, the curve of RSS variation becomes narrower when a human is present.

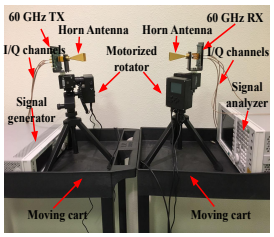

Figure 6: 60 GHz sensing system.

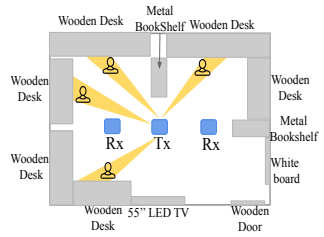

Figure 7: Illustration of indoor environment.

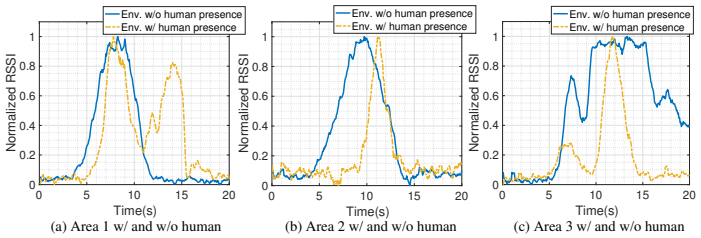

Figure 8: Examples of RSS traces in environment with and without human presence.

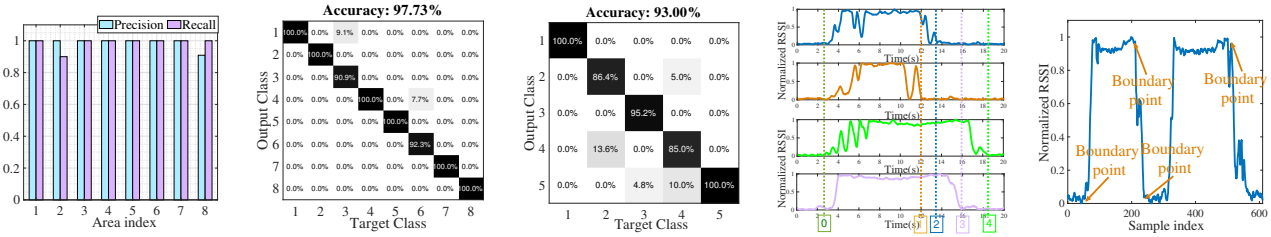

Figure 9: (a) Precision and recall for 8 areas w/o human presence. (b) Confusion matrix for 4 areas w/ and w/o human presence. (c) Confusion matrix for 5 person classification. (d) Measurement of different person's chest breadth. (e) Construction of human outline via finding boundary points.

The reason is that this is a corner area, and the human body blocks part of the second order reflected beams. From Figure 8c, we can see that the fingerprint of this area with human presence is different from the other two areas, which implies a more complicated environment.

In order to implement human detection and localization, we have to prove that the environment with and without human presence can be fingerprinted. First, we show that without human presence, the environment is distinguishable. And then, we can further distinguish the environments with and without human presence. We split the environment shown in Figure 7 into 8 areas and collect 35 sequential RSS samples for each area. Each RSS ample consists of 600 RSS data points and form the fingerprint of the area. Then we import the data into the LSTM neural network to train and test and obtain a classification accuracy of 98.75%, which is displayed in Figure 9a. Further, we collect the fingerprints of the environments with human presence. We use the fingerprints to determine in which areas humans are present. Then we can detect the multi-person human presence and their locations. Figure 9b displays the confusion matrix for four areas with and without human presence. The classification accuracy can reach to 97.73%, which also shows the excellent performance of human detection and localization. Figure 7 shows our approach finally detects four persons and their locations, which match the fact that four people sit in the office.

Human identification. Once a human is located, Tx and Rx adjust their beams towards the human body, and we attempt to identify the person. We conduct some preliminary experiments to show the effectiveness of our approach. We propose a rich feature set to identify humans. First, we evaluate the vital signs related features. We recruit five volunteers to assist in our experiments. We make the Tx and Rx towards these volunteers' chest and collect 90 samples for each person. Each sample consists of an RSS sequence of 30 seconds. We process the data using a 12s sliding window and extract 14 statistic features(e.g., mean and std) for each window. Then we use a random forest classifier to classify the five people and obtain an accuracy of 93%. The confusion matrix of the classification is shown in Figure 9c.

Another feature we utilize is the human outline. As shown in Figure 3, we use the 60 GHz reflection signals to measure the human body' width. We measure four people's bust width and show the monitored RSS sequence in Figure 9d. The marker [0] displays the left boundary points of four people, which is the start of the reflected signal. We can see the other four different markers in the feature representing the right boundary points of different people. The widths of the reflected signal indicate the chest widths of different people.

Moreover, we want to construct the human outline, not just the chest width. Figure 9e shows the idea of constructing the human outline by continuously finding boundary points of the body. We first scan the body horizontally until the beam touches the human body(first reflected signal), then vertically move the TX beam direction and scan horizontally in the direction opposite to the previous horizontal scan until the TX beam moves out human body (no reflected signal). The first two boundary points in Figure 9e show this procedure. We repeat this procedure and scan the human body along a modified zigzag route. The density of boundary points determines the granularity of the human body outline.

Fine-grained outline makes high identification accuracy but also incurs the higher processing overhead. We plan to thoroughly explore the relationship between point density, construction cost and identification accuracy in *future work*.

4 RELATED WORK

In recent years, many research work about algorithms, protocols, frameworks, and applications [5, 6, 9, 15] about mmWave communication greatly enhance the broad deployment of mmWave devices. The very short wavelength, high directionality, and good reflectivity lead to a unique sensing property of mmWave signal. [12] harnesses 60 GHz radios to sense the environment to boost network performance. [18] uses only RSS series analysis to sense and image an object. Authors in [16] studies the feasibility of using mmWave to sense sugar contents in fruits. WaveEar [14] can recover the voice by directing the mmWave signals towards the near-throat region of the speaker and sensing his/her vocal vibrations. The excellent sensing capabilities of mmWave provide us a new chance to implement multi-person detection and identification.

In numerous scenarios, such as smart home and smart industry, detecting human presence, localizing their positions, and further identifying are the fundamental services for applications. WiFi radio is widely adopted in human sensing. [8] detects the human presence via analyzing occurrences of non-linear correlations among subcarriers. In order to degrade multipath effects, [10] tries to pre-process the CSI data and utilizes the subcarriers' data that are not affected by multipath to increase the accuracy of human detection and localization. The amplitude and phase information of CSI is also leveraged to detect human's vital signs and gait pattern [1, 4, 13] to identify and authenticate users. However, these methods cannot detect and identify multiple people due to the strict environment requirement for WiFi sensing. *mmSense* uses mmWave signal' high sensitivity to human body and unique spatial isolation to greatly release the environment constrains while increasing the human detection and identification accuracy.

5 CONCLUSION

In this work, we propose *mmSense* a novel approach that leverages mmWave sensing to implement human detection and identification. The traditional methods have a variety of drawbacks. The visible light imaging system(e.g. cameras) cannot work in dark or low-light conditions and require massive computation power. The WiFi-based sensing technique requires controlled environments and cannot detect multiple people. *mmSense* can detect and localize the presences of multiple people simultaneously by using 60 GHz signals to fingerprint the environments with and without human presence. Moreover, we propose a novel approach that uses humans' outline profile and vital signs to identify multiple people by using 60 GHz reflected signals of the human body. We conduct extensive experiments to demonstrate the effectiveness of our approach.

REFERENCES

[1] Heba Abdelnasser, Khaled A Harras, and Moustafa Youssef. 2015. UbiBreathe: A ubiquitous non-invasive WiFi-based breathing estimator. In *MobiHoc'15*. ACM, 277–286.

[2] J. Ahmadi-Shokouh, S. Noghanian, E. Hossain, M. Ostadrahimi, and J. Dietrich. 2009. Reflection Coefficient Measurement for House Flooring Materials at 57-64 GHz. In *GLOBECOM'09*. 1–6.

[3] Aveek K Das, Parth H Pathak, Josiah Jee, Chen-Nee Chuah, and Prasant Mohapatra. 2017. Non-intrusive multi-modal estimation of building occupancy. In *SenSys'17*. ACM.

[4] Biyi Fang, Nicholas D Lane, Mi Zhang, Aidan Boran, and Fahim Kawsar. 2016. BodyScan: Enabling radio-based sensing on wearable devices for contactless activity and vital sign monitoring. In *MobiSys'16*. ACM.

[5] Yasaman Ghasempour, Muhammad K Haider, Carlos Cordeiro, Dimitrios Koutsonikolas, and Edward Knightly. 2018. Multi-stream beam-training for mmWave MIMO networks. In *MobiCom'18*. ACM.

[6] Tianbo Gu, Zhicheng Yang, Debraj Basu, and Prasant Mohapatra. 2019. BeamSniff: Enabling Seamless Communication under Mobility and Blockage in 60 GHz Networks. In *2019 IFIP Networking Conference (IFIP Networking)*. IEEE.

[7] Hessam Mohammadmoradi, Shengrong Yin, and Omprakash Gnawali. 2017. Room occupancy estimation through wifi, UWB, and light sensors mounted on doorways. In *ICSDE'17*. ACM, 27–34.

[8] Sameera Palipana, Piyush Agrawal, and Dirk Pesch. 2016. Channel State Information Based Human Presence Detection Using Non-linear Techniques. In *BuildSys'16*. ACM, 177–186.

[9] Sanjib Sur, Ioannis Pefkianakis, Xinyu Zhang, and Kyu-Han Kim. 2018. Towards scalable and ubiquitous millimeter-wave wireless networks. In *MobiCom'18*. ACM, 257–271.

[10] Ju Wang, Hongbo Jiang, Jie Xiong, Kyle Jamieson, Xiaojiang Chen, Dingyi Fang, and Binbin Xie. 2016. LiFS: low human-effort, device-free localization with fine-grained subcarrier information. In *MobiCom'16*. ACM, 243–256.

[11] Wei Wang, Alex X. Liu, Muhammad Shahzad, Kang Ling, and Sanglu Lu. 2015. Understanding and Modeling of WiFi Signal Based Human Activity Recognition. In *MobiCom'15*. ACM, 65–76.

[12] Teng Wei, Anfu Zhou, and Xinyu Zhang. 2017. Facilitating robust 60 ghz network deployment by sensing ambient reflectors. In *NSDI'17*. 213–226.

[13] C. Wu, Z. Yang, Z. Zhou, X. Liu, Y. Liu, and J. Cao. 2015. Non-Invasive Detection of Moving and Stationary Human With WiFi. *IEEE Journal on Selected Areas in Communications* 33, 11 (Nov 2015), 2329–2342.

[14] Chenhan Xu, Zhengxiong Li, Hanbin Zhang, Aditya Singh Rathore, Huining Li, Chen Song, Kun Wang, and Wenyao Xu. 2019. WaveEar: Exploring a mmWave-based Noise-resistant Speech Sensing for Voice-User Interface. In *MobiSys'19*. ACM, 14–26.

[15] Zhicheng Yang, Parth H Pathak, Jianli Pan, Mo Sha, and Prasant Mohapatra. 2018. Sense and deploy: Blockage-aware deployment of reliable 60 ghz mmwave wlans. In *IEEE MASS'18*. IEEE, 397–405.

[16] Zhicheng Yang, Parth H Pathak, Mo Sha, Tingting Zhu, Junai Gan, Pengfei Hu, and Prasant Mohapatra. 2019. On the feasibility of estimating soluble sugar content using millimeter-wave.. In *ACM/IEEE IoTDI'19*. 13–24.

[17] Zhicheng Yang, Parth H Pathak, Yunze Zeng, Xixi Liran, and Prasant Mohapatra. 2016. Monitoring vital signs using millimeter wave. In *MobiHoc'16*. ACM, 211–220.

[18] Yanzi Zhu, Yibo Zhu, Ben Y Zhao, and Haitao Zheng. 2015. Reusing 60ghz radios for mobile radar imaging. In *MobiCom'15*. ACM, 103–116.

[19] Han Zou, Yuxun Zhou, Jianfei Yang, Weixi Gu, Lihua Xie, and Costas J Spanos. 2018. Wifi-based human identification via convex tensor shapelet learning. In *AAAI'18*.